Journal of Sol-Gel Science and Technology (2019) 92:208–214
https://doi.org/10.1007/s10971-019-05076-2

ORIGINAL PAPER: SOL–GEL AND HYBRID MATERIALS FOR CATALYTIC, PHOTOELECTROCHEMICAL AND SENSOR APPLICATIONS

Sol–gel synthesis and characterization of the binary Ni–Mg–O oxide system

Timofey M. Karnaukhov[1,2] · Aleksey A. Vedyagin[1] · Svetlana V. Cherepanova[1,2] · Vladimir A. Rogov[1,2] · Ilya V. Mishakov[1,2]

Received: 18 February 2019 / Accepted: 9 July 2019 / Published online: 16 July 2019

Abstract

In this work, the binary Ni–Mg–O oxide system was prepared by means of a sol–gel technique, which provides high dispersity and uniform distribution of the nickel species within the MgO matrix. The samples were characterized by a scanning electron microscopy, a low-temperature nitrogen adsorption, and X-ray diffraction analysis. The reducibility of the prepared samples was tested in the reduction/oxidation cycles, thus modeling the conditions of a chemical looping. It was found that during the preparation procedure, a partial substitution of Mg^{2+} ions with Ni^{2+} ions resulting in formation of solid solution takes place. Reduction of the as-prepared sample in a temperature-programmed regime with heating up to 700 °C leads to decomposition of the solid solution and formation of dispersed particles of metallic nickel of 7 nm in size finely distributed within the MgO matrix. Subsequent oxidation transforms Ni^0 species into NiO nanoparticles. Starting from the second reduction/oxidation cycle, the binary Ni–Mg–O system shows the reproducible behavior, and thus can be considered as a chemical looping agent.

Graphical Abstract

The binary Ni-Mg-O oxide system was synthesized by modified sol-gel technique, when hydrolysis of $Mg(OCH_3)_2$ was performed using aqueous solution of nickel nitrate instead of pure water. The calcined samples are characterized with high dispersity and uniform distribution of the nickel species within the MgO matrix. The reducibility of the prepared samples in the reduction/oxidation cycles was found to be reproducible starting from the second cycle.

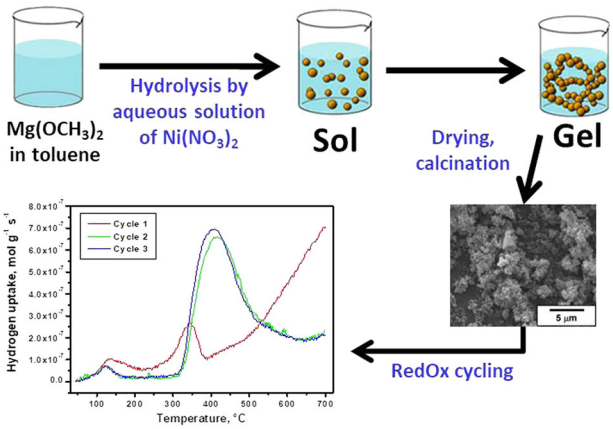

✉ Aleksey A. Vedyagin
vedyagin@catalysis.ru

[1] Boreskov Institute of Catalysis, Siberian Branch, Russian Academy of Sciences, 630090 Novosibirsk, Russian Federation

[2] National Research University–Novosibirsk State University, 630090 Novosibirsk, Russian Federation

Highlights

- The binary Ni–Mg–O oxide system was prepared by means of a sol–gel technique.
- MgO was shown to strongly affect the reducibility of NiO.
- A partial substitution of Mg^{2+} ions with Ni^{2+} ions takes place.
- Decomposition of the solid solution in a hydrogen flow occurs at 700 °C.
- Nanoparticles of metallic nickel finely distributed within MgO were formed.

Keywords Nanostructured MgO Doping · Nickel oxide · Characterization · Reducibility

1 Introduction

Nickel oxide attracts a great attention to be applied as a component of the catalysts, sensors, batteries, etc. [1–9]. On the other hand, NiO-based systems can be considered as an oxygen storage material. Such materials are able to allot oxygen in a reductive medium, and thus can be used in the chemical looping processes, like deep oxidation of the hydrocarbons, alkane dehydrogenation, and others [10]. During the oxidative regeneration procedure, it can easily reduce its initial oxidized state. Thereby, the study on the reduction behavior of the NiO-based systems is quite important for the mentioned applications.

The reduction of nickel oxide depending on the reaction conditions is known to proceed in a temperature range of 150–300 °C [11, 12]. An increase of the particle size leads to shifting the reduction temperature range toward higher temperatures [11]. Both the samples with low (1 m^2/g) and developed (57 m^2/g) specific surface area (SSA) show two hydrogen consumption peaks. The intensities of these peaks correlate well with the mentioned particle sizes: reduction of the disperse surface NiO takes place at lower temperatures, while the bulk NiO reduces in a high-temperature region. It was also shown that an increase of the ramping rate shifts the reduction temperature interval toward elevated temperatures. As reported in [12], presence of the water vapors in a reaction volume additionally complicates the reduction process. Another important factor affecting reducibility of the nickel oxide system is a presence of organic and inorganic impurities or additives. As an example, the impurities of chloride or acetate anions negatively change the rate of NiO reduction [13]. An addition of a small amount of precious metals (Pt, Pd) accelerates the reduction process due to increased efficiency of a hydrogen spillover [13, 14]. Platinum and palladium atoms are able to absorb hydrogen and transfer it to nickel oxide.

NiO is also known to be inclined to strong interaction with oxides of other metals. In some cases, it facilitates the reduction process performed in a hydrogen stream. As it was reported by Pospišil for the NiO–CeO_2 system [15], nickel oxide is reduced with noticeably increased rate. The similar situation was observed for the NiO–Co_3O_4 binary oxide system [16]. An increase of the cobalt oxide content leads to an acceleration of the reduction process, and the rate of reduction goes through a maximum at 16 wt.% of NiO. Thereby, in this case, positive synergetic effect of nickel and cobalt oxides interaction is observed, when the joint oxide system is being reduced easily if compared with pristine NiO and Co_3O_4. At the same time, in a majority of the cases, oxide supports complicate the reduction of NiO [8, 11, 12, 17–20]. As it is shown in ref. [11], depending on the NiO–Al_2O_3 ratio the temperature range of a hydrogen uptake can be shifted from 200–300 °C for pure NiO to 800–900 °C for NiO/Al_2O_3 with a molar ratio of 1:7. Calcination of this system at 1000 °C strengthens the interaction of oxides and shifts the reduction temperature range more significantly. The analogous effects were found for the mixed oxide $NiTiO_3$ and $NiCr_2O_4$ systems [12]. The reduction of NiO–YSZ (where YSZ is yttria-stabilized zirconia), which is considered as a perspective material to be used in fuel cells, proceeds via multistage route with hardly separable peaks within a temperature range of 400–700 °C [17]. Diminishing the reduction rate due to the interaction of NiO with the difficult-to-reduce oxides (ZnO, V_2O_5, ThO_2) at the constant reduction temperature was described in refs. [14, 18, 19].

Another important feature of nickel oxide is its disposition toward very strong interaction with magnesium oxide. The values of ionic radius for Ni^{2+} and Mg^{2+} are practically coincided (0.078 Å), which leads to the formation of solid solutions of substitution. As a rule, the reduction of such joint phases is complicated if compared with pristine NiO. As an example, addition of 1–2 wt.% MgO to alumina-supported NiO (10 wt.%) significantly increases the activation energy of the NiO reduction with hydrogen, and shifts the reduction temperature range to higher temperatures (on about 400 °C) [20]. It is also known that an enlargement of the MgO–NiO ratio in the two-component oxide system rises the degree of nickel cations bonding within the MgO matrix [21, 22]. All this is reflected in the corresponding reduction profiles: the hydrogen consumption peaks are getting broader and become shifted toward elevated temperatures. The value of the relative reduction degree was also found to be diminished with an increase of the MgO–NiO ratio.

Taking into account all mentioned above, it can be concluded that the process of NiO reduction with

hydrogen can be easily controlled by an addition of different oxide modifiers. An appropriate composition of the binary oxide system allows one to obtain the desired reduction degree within the desired reduction temperature range. In these terms, the binary Ni–Mg–O system looks very promising, and can be considered as a main chemical looping component for the dehydrogenation processes, where both the hydrogen release and controllable uptake are involved. This work continues the series of research papers devoted to the study of the MgO-based binary systems derived via a sol–gel technique [23–27]. The used approach provides a high dispersity of the nickel species, their uniform distribution within the MgO matrix and good enough stability in the consecutive reduction/oxidation cycles. Here, the MgO-based system containing 15 wt.% of NiO was prepared, characterized by a set of the physicochemical methods, and tested in terms of its reduction with hydrogen.

2 Experimental

2.1 Synthesis of the samples

A two-component Ni–Mg–O oxide system was prepared by means of a sol–gel technique, as described elsewhere [24]. A sample of magnesium metal ribbon (Aldrich, USA, 99.9%, 0.15 mm, 1 g) was cut into small pieces and blended with dry methanol (30 ml). Then, toluene was added as a gel stabilizer. Methanol to toluene volume ratio was 1:1. The obtained magnesium methoxide was hydrolyzed dropwise by a water solution of nickel (II) nitrate hexahydrate (1.2 M, 1.5 ml) at a room temperature during 1 h. The formed gel was dried at a room temperature during 2 h, and at 200 °C during another 2 h. In order to obtain Ni–Mg–O oxide, the xerogel was calcined stepwise by heating from a room temperature to 300 °C with a ramping rate of 5 °C/min, heating to 400 °C with rate of 1 °C/min, and, finally, heating to 500 °C with rate of 5 °C/min. The nickel loading was 15 wt.% in regard to NiO. Reference MgO sample was prepared similarly with the only exception that the magnesium methoxide was hydrolyzed dropwise by distilled water. Pure nickel oxide used as another reference sample was obtained by decomposition of nickel (II) nitrate hexahydrate at step-by-step heating up to 500 °C.

2.2 Characterization of the samples

The SSA of the samples was measured by the BET method using a low-temperature nitrogen adsorption. The pore size distributions were determined from the nitrogen adsorption isotherms at 77 K using ASAP-2400 (Micrometrics, USA) and Digisorb–2600 instruments (Quantochrome, USA).

The texture of the Ni–Mg–O samples was studied using a JSM-6460 (Jeol, Japan) scanning electron microscope in both the SE and BSE modes. The microscope ensured magnifications from ×8 to ×300.000.

Powder X-ray diffraction (XRD) analysis of the samples was performed in an in situ regime under reductive and oxidative atmospheres using a diffractometer D8 (Bruker, Germany). Initially, the sample was in situ reduced in a hydrogen flow at heating up to 700 °C. Then, it was cooled down to room temperature (25 °C) in a hydrogen flow, passivated in helium at 25 °C, and then oxidized in a gas flow containing 5 vol.% oxygen in helium at heating up to 700 °C. Finally, the sample was cooled down to 25 °C in the same gas mixture. A ramping rate was 10 °C/min. A gas flow rate in all experiments was 20 ml/min. Diffraction patterns were registered at 25, 300, 500, and 700 °C within an angle range of 15–85°, with a step of 0.05° and accumulation time of 3 s in each point. Cell parameters were determined using the patterns obtained at a room temperature only (without thermal expansion). All calculations were carried out using a software TOPAS (Bruker, Germany).

2.3 Study on reduction behavior

The reduction behavior of the Ni–Mg–O oxide system was studied using a temperature-programmed reduction (TPR) method. The sample was heated up in a hydrogen-containing flow (10 vol.% H_2 in argon; gas flow rate: 40 ml/min) within a temperature range of 50–900 °C with a ramping rate of 10 °C/min. Before the experiments, each sample was kept in an argon flow at 150 °C in order to remove adsorbed water. Hydrogen concentration was measured by a thermal conductivity detector (current: 70 mA). A standardized sample CuO was used for calibration to calculate the hydrogen uptake in $\mathrm{mol} \times \mathrm{g}^{-1} \times \mathrm{s}^{-1}$.

In addition, the sample of Ni–Mg–O binary oxide was examined in a periodic reduction/re-oxidation regime. In each cycle, the sample was subjected to a thermal treatment in air flow before the reduction stage. The sample was heated from room temperature to 500 °C with a ramping rate of 20 °C/min, and was kept at 500 °C for 30 min. The reduction stage was performed similarly to that described above, but with a final temperature of 700 °C.

3 Results and discussion

The as-prepared binary Ni–Mg–O oxide system was characterized by means of a scanning electron microscopy and low-temperature nitrogen adsorption. As it follows from SEM images presented in Fig. 1, the morphology of the sample remains that for pure MgO. The sample is represented by the chaotically adherent agglomerates of the

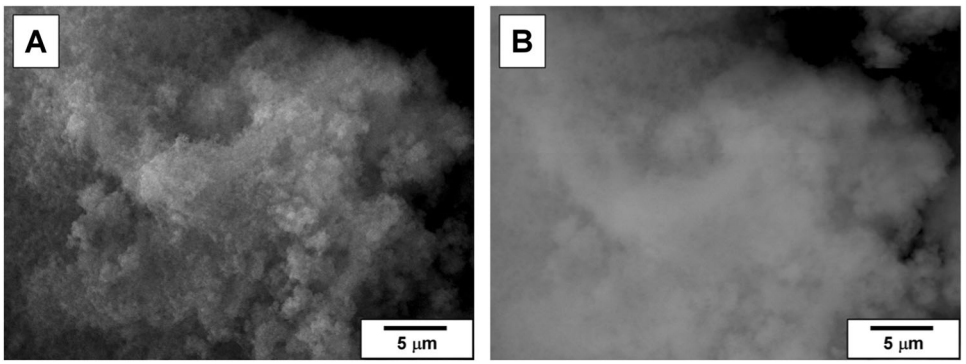

Fig. 1 SEM images for the as-prepared Ni–Mg–O sample: SE mode (**a**), BSE mode (**b**)

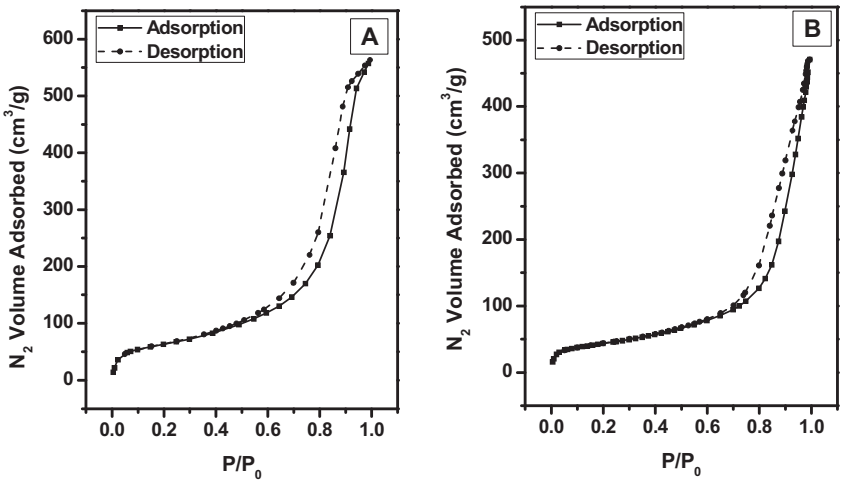

Fig. 2 Type IV isotherms for the reference MgO sample (**a**) and the as-prepared Ni–Mg–O sample (**b**)

primary smaller particles (Fig. 1a). No unusual substructuring was observed in this case. SEM image obtained in a backscattered electrons mode (Fig. 1b) confirms that nickel species are quite small and evenly distributed within the MgO matrix. Figure 2 compares the type IV isotherms for the pure MgO sample and the binary Ni–Mg–O system. According to the results of a low-temperature nitrogen adsorption, introduction of nickel oxide into the MgO matrix diminishes the value of SSA from 243 m^2/g for pure MgO to 154 m^2/g for the Ni–Mg–O sample. The average pore diameter changes correspondingly: from 61 Å to 189 Å. Despite the difference in density of magnesium and nickel oxides (3.58 and 6.67 g/cm^3, correspondingly), the main reason of observed worsening of the textural characteristics is supposed to be an effect of a presence of nickel nitrate during the sol-formation process.

The reducibility of the Ni–Mg–O system was studied by means of a TPR technique. Figure 3a shows the TPR profiles for the binary oxide sample along with a reference sample—bulk NiO prepared via calcination of the same precursor. The intensity of the hydrogen uptake for the Ni–Mg–O sample was normalized in relation to the NiO content. As seen from the profiles, in the case of bulk NiO, the reduction process goes through one stage with a maximum at 380 °C, which corresponds to a phase transition of NiO to metallic Ni. In contrast, reduction of the binary Ni–Mg–O system, when NiO species are considered to be uniformly distributed within the MgO matrix, gives more complicated picture. There are three hydrogen uptake peaks clearly seen on the TPR profile. The first peak (200–350 °C) can be assigned to the reduction of the surface NiO species having weak interaction with MgO. Then follows the peak at 370–500 °C corresponding to the reduction of the similar NiO species distributed in the bulk of the MgO matrix, which is slightly complicated by hydrogen diffusion. Finally, the largest and widest peak is appeared at 500–890 °C. The appearance of this peak is connected with reduction of strongly bonded nickel species formed due to substitution of Mg^{2+} ions with Ni^{2+} ions. Thereby, the effect of the MgO matrix on the reduction behavior of nickel oxide is evident and significant.

The results of the reduction/oxidation cycling for the binary Ni–Mg–O oxide sample are presented in Fig. 3b. As seen, the TPR profiles for the first and subsequent cycles are noticeably different. In the case of the first cycle, reduction of the NiO proceeds through the stages described above. In addition, an appearance of a new low-temperature peak (100–150 °C) is observed. Since in these experiments the

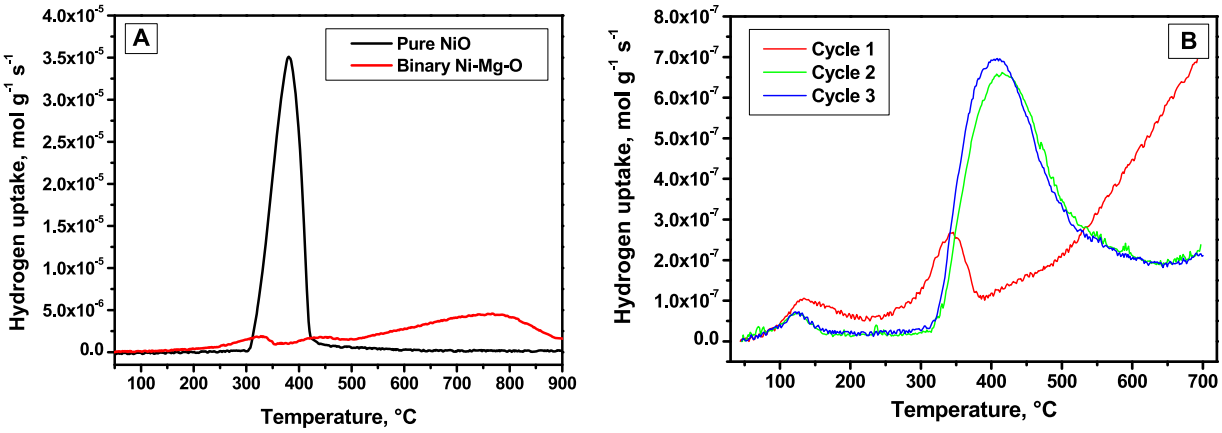

Fig. 3 TPR profiles for the Ni–Mg–O sample and pure nickel oxide (**a**), and for the Ni–Mg–O sample in three consecutive oxidation/reduction cycles (**b**)

sample was pretreated in air flow, the peak can be attributed to the reduction of the surface hydroxyl groups being formed. Starting from the second cycles, only two hydrogen uptake peaks are well seen. Besides the low-temperature peak, the second peak assigned to reduction of the NiO nanoparticles within the MgO matrix is present and makes the main contribution to the total hydrogen uptake. The intensity of this peak is evidently increased if compared with the same peak in the profile for the first cycle. It testifies that part of the strongly bonded nickel species left their substitution positions in the MgO lattice during the reduction procedure with formation of metallic Ni. Then, during the re-oxidation stage, metallic Ni was transformed into NiO nanoparticles located in the bulk of MgO. Both the dispersity and uniform distribution of NiO within the MgO matrix are believed to remain the same. In the third reduction cycle, the TPR profile almost completely reproduces the previous one. Slight increase of intensity of the second peak indicates that additional small part of strongly bonded nickel species was converted into dispersed NiO nanoparticles during the second reduction/oxidation cycle. Thereby, it can be concluded that the binary Ni–Mg–O oxide system starts to work reproducibly in the reduction/oxidation cycles within the temperature range of 50–700 °C after the first cycle. Significant changes of the phase composition taking place during the first cycle under the action of reaction medium at elevated temperature lead to an alteration of the reduction behavior of the NiO distributed within the MgO matrix. In order to confirm the suppositions made, the binary oxide sample was studied by an in situ XRD analysis (Fig. 4). The quantitative results of XRD analysis are summarized in Table 1. The XRD pattern for the as-prepared binary Ni–Mg–O oxide system contains only the peaks corresponding to solid solution of NiO and MgO [22, 25]. Heating the sample in a hydrogen flow results in an increase of the MgO crystallites reflected in a

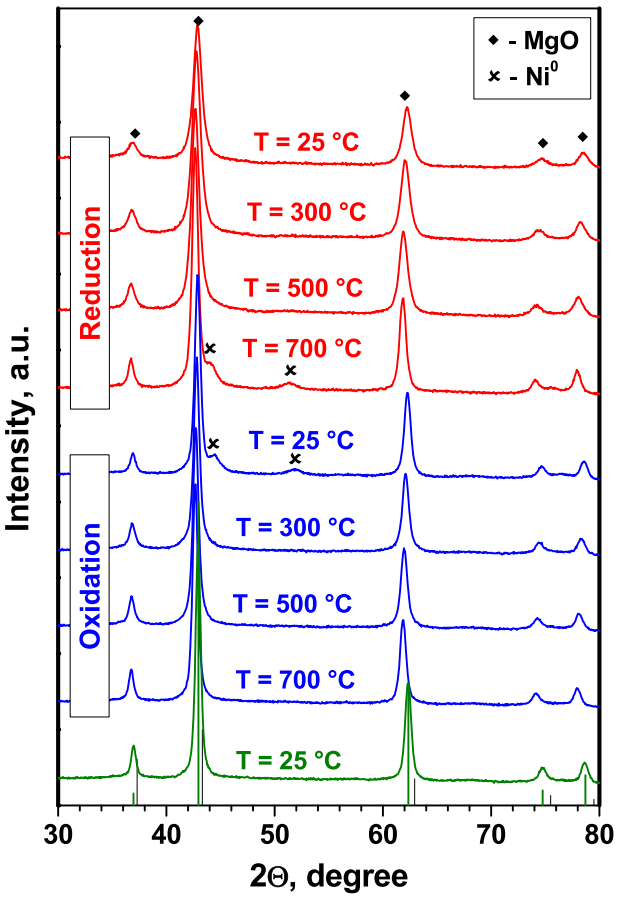

Fig. 4 In situ XRD patterns for the Ni–Mg–O oxide sample after heating in the reductive atmosphere, after heating in the oxidative atmosphere, and after e cooling down to room temperature

narrowing of the peaks in the pattern. Appearance of the peaks assigned to Ni^0 was observed at 700 °C, thus testifying toward decomposition of the solid solution and formation of dispersed Ni nanoparticles within the MgO matrix at elevated temperatures. These peaks rapidly disappear

Table 1 Quantitative results of an in situ XRD analysis

Phase	Initial		Reduced		Oxidized	
	a, Å	D_{av}, nm	a, Å	D_{av}, nm	a, Å	D_{av}, nm
MgO	4.221 (1)	7	4.217 (1)	12	4.215 (1)	13
Ni	–	–	3.522 (2)	7	–	–

during the heating the sample in an oxidative medium. The size of Ni nanoparticles was estimated to be 7 nm.

It should be noted that according to the JCPDS-ICDD database, the lattice parameter for pure bulk MgO is equal to 4.211 Å (PDF#45-0946). In the case of samples obtained via a sol–gel technique, this parameter can be noticeably increased up to 4.227–4.233 Å [28]. As it follows from the obtained results, high-temperature treatment leads to an enlargement and crystallization of the MgO particles. The lattice spacing progressively decreases approaching to the mentioned reference value for magnesium oxide crystals. Effect of the nickel species distributed within the MgO matrix is seemed to be negligible.

The differences in the reduction behavior in the first and consecutive TPR cycles can be explained by the different strength of interaction between NiO and MgO. During the first reduction cycle, nickel species strongly bonded with the MgO matrix undergo reduction at temperature near 700 °C, which results in formation of metallic Ni of 7 nm in size. The subsequent oxidation of the dispersed metallic particles leads to formation of NiO nanoparticles, while no ionic substitution along with formation of the NiO–MgO solid solution takes place. Thereby, starting from the second reduction/oxidation cycle, the binary Ni–Mg–O oxide system behaves reproducibly with a hydrogen uptake at 350–550 °C corresponding to the reduction of NiO to Ni^0.

4 Conclusions

A sol–gel approach was applied to prepare the binary Ni–Mg–O oxide system. Nickel oxide species were shown to be uniformly distributed within the MgO matrix. Partial substitution of Mg^{2+} ions with Ni^{2+} ions takes place at the used preparation conditions. All these significantly affects the reducibility of nickel oxide. At least two types of nickel species were found to be present in the binary oxide sample: weakly bonded NiO nanoparticles uniformly distributed within the MgO matrix and strongly bonded nickel species formed via the substitution of Mg^{2+} ions with Ni^{2+} ions. Heating the Ni–Mg–O sample up to 700 °C in a reducing medium (hydrogen flow) results in decomposition of the NiO–MgO solid solution with formation of metallic Ni nanoparticles of 7 nm distributed in the bulk of MgO. The following oxidation/reduction cycles are reproducible, and the main hydrogen uptake takes place within the temperature interval of 350–550 °C.

Funding This study was supported by the Ministry of Science and High Education of Russian Federation (projects AAAA-A17-117041710079-8 and AAAA-A17-117041710086-6).

Compliance with ethical standards

Conflict of interest The authors declare that they have no conflict of interest.

Publisher's note: Springer Nature remains neutral with regard to jurisdictional claims in published maps and institutional affiliations.

References

1. Tadic M, Panjan M, Markovic D (2010) NiO/SiO_2 nanostructure and the magnetic moment of NiO nanoparticles. Mat Lett 64:2129–2131
2. Nassar N, Hassan A, Pereira-Almao P (2012) Thermogravimetric studies on catalytic effect of metal oxide nanoparticles on asphaltene pyrolysis under inert conditions. J Therm Anal Calor 110:1327–1332
3. Khairy M, El-Safty S, Ismael M, Kawarada H (2012) Mesoporous NiO nanomagnets as catalysts and separators of chemical agents. Appl Catal B-Environ 127:1–10
4. Wei W, Cui B, Jiang X, Lu L (2010) The catalytic effect of NiO on thermal decomposition of nitrocellulose. J Therm Anal Calor 102:863–866
5. Wang N, Liu C, Wen B, Wang H, Liu S, Chai W (2014) Enhanced optical and electrical properties of NiO thin films prepared by rapid radiation pyrolysis method based on the sol–gel technique. Mat Lett 122:269–272
6. Wang Q, Zhang C, Shan W, Xing L, Xue X (2014) Uniformly loading NiO nanowalls on graphene and their extremely high capacity and cyclability as anodes of lithium-ion batteries. Mat Lett 118:66–68
7. Stefanescu M, Sorescu S, Susan-Resiga D, Stefanescu O, Vlase G (2015) Obtaining of NiO/SiO_2 by thermal decomposition of Ni(II) carboxylates formed within hybrid silica gels. J Therm Anal Calor 121:135–144
8. Zare M, Ketabchi M (2017) Effect of chromium element on transformation, mechanical and corrosion behavior of thermo-mechanically induced Cu–Al–Ni shape-memory alloys. J Therm Anal Calor 127:2113–2123
9. Bahari Mollamahale Y, Liu Z, Zhen Y, Tian ZQ, Hosseini D, Chen L, Shen PK (2017) Simple fabrication of porous NiO nanoflowers: growth mechanism, shape evolution and their application into Li-ion batteries. Int J Hydrog Energ 42:7202–7211
10. Adanez J, Abad A, Garcia-Labiano F, Gayan P, de Diego LF (2012) Progress in chemical-looping combustion and reforming technologies. Prog Energ Combust Sci 38:215–282

11. Soboleva TN, Rudnitsky LA, Alekseyev AM (1980) Thermogravimetry of the NiO-Al_2O_3 system in a hydrogen flow. J Therm Anal 18:517–525
12. Goldman DB (1985) Evolved gas analysis for examination of surface oxides on alloys. J Therm Anal 30:1071–1080
13. Pospišil M, Kaňoková P (1999) Effect of different treatment on the reducibility of NiO-Y_2O_3 mixed oxides by hydrogen. J Therm Anal Calor 58:77–88
14. Pospišil M, Cuba V, Poláková D (2004) Effect of genesis on the properties and hydrogen reducibility of NiO–ZnO mixed oxides. J Therm Anal Calor 75:35–50
15. Pospišil M (1984) Effects of genesis and ionizing radiation on the kinetics of reduction of NiO-CeO_2 mixed oxides with hydrogen. J Therm Anal 29:49–59
16. Pospišil M (1990) Physico-chemical properties and hydrogen reduction reactivity of nickel and cobalt mixed oxides of various stoichiometry. J Therm Anal 36:489–502
17. Yoshito WK, Matos JR, Ussui V, Lazar DRR, Paschoal JOA (2009) Reduction kinetics of NiO–YSZ composite for application in solid oxide fuel cell. J Therm Anal Calor 97:303–308
18. Pospišil M (1983) Study of reduction kinetics of mixed oxides NiO-V_2O_5 with hydrogen. J Therm Anal 27:77–88
19. Pospíšil M, Hosek R, Silber R (2001) Properties of NiO-ThO_2 mixed oxides from hydroxides and their hydrogen reducibility behavior. J Therm Anal Calor 66:449–461
20. Richardson JT, Scates RM, Twigg MV (2004) X-ray diffraction study of the hydrogen reduction of NiO/α-Al_2O_3 steam reforming catalysts. Appl Catal A-Gen 267:35–46
21. Zanganeh R, Rezaei M, Zamaniyan A (2013) Dry reforming of methane to synthesis gas on NiO-MgO nanocrystalline solid solution catalysts. Int J Hydrog Energ 38:3012–3018
22. Wang Y, Yang X, Wang Y (2016) Catalytic performance of mesoporous MgO supported Ni catalyst in steam reforming of model compounds of biomass fermentation for hydrogen production. Int J Hydrog Energ 41:17846–17857
23. Mishakov IV, Ilyina EV, Bedilo AF, Vedyagin AA (2009) Nanocrystalline aerogel VOx/MgO as a catalyst for oxidative dehydrogenation of propane. Reac Kinet Catal Lett 97: 355–361
24. Vedyagin AA, Mishakov IV, Karnaukhov TM, Krivoshapkina EF, Ilyina EV, Maksimova TA, Cherepanova SV, Krivoshapkin PV (2017) Sol-gel synthesis and characterization of two-component systems based on MgO. J Sol-Gel Sci Technol 82:611–619
25. Karnaukhov TM, Vedyagin AA, Cherepanova SV, Rogov VA, Stoyanovskii VO, Mishakov IV (2017) Study on reduction behavior of two-component Fe-Mg-O oxide system prepared via a sol-gel technique. Int J Hydrog Energ 42:30543–30549
26. Karnaukhov T, Vedyagin A, Mishakov I, Bedilo A, Volodin A (2018) Synthesis and characterization of nanocrystalline M-Mg-O and carbon-coated MgO systems. Mater Sci Forum 917:157–161
27. Vedyagin AA, Karnaukhov TM, Cherepanova SV, Stoyanovskii VO, Rogov VA, Mishakov IV (2018) Synthesis of binary Co-Mg-O oxide system and study of its behavior in reduction/oxidation cycling. Int J Hydrogen Energ https://doi.org/10.1016/j.ijhydene.2018.05.044
28. Bedilo AF, Shuvarakova EI, Volodin AM, Ilyina EV, Mishakov IV, Vedyagin AA, Chesnokov VV, Heroux DS, Klabunde KJ (2014) Effect of modification with vanadium or carbon on destructive sorption of halocarbons over nanocrystalline MgO: the role of active sites in initiation of the solid-state reaction. J Phys Chem C 118:13715–13725